ICSV13 - Vienna
The Thirteenth International Congress on Sound and Vibration
Vienna, Austria, July 2-6, 2006

COMPARISON OF DIFFERENT ACTUATOR CONFIGURATIONS FOR ACTIVE ISOLATION OF CAR ENGINE INDUCED VIBRATION REGARDING POWER CONSUMPTION

Jörg Paschedag* and Guido Koch

Institute of Automatic Control (Prof. Dr.-Ing. habil. B. Lohmann),
Technical University Munich
Boltzmannstr. 15, Germany - 85748 Garching / Munich
paschedag@tum.de

Abstract

Concern of this paper is the energy-saving arrangement of force actuators in an active vibration control system. The considered application is active vibration isolation in an automobile: To improve the ride comfort, the engine induced vibration is to be kept off the chassis. Six different configurations of actuator placement in the engine mounting are analyzed regarding their power demands. Therefore models of the overall setup are derived and algebraic frequency dependent formulas for the calculation of average mechanical and electrical power consumption are deduced. The results of the analysis are evaluated and compared to measurement data of an experimental car setup.

1. INTRODUCTION

The cancellation of disturbing machinery vibration is current concern of research and industrial development [1]. One important application regarding this matter is the isolation of engine induced vibration in automobiles [2]. Subject of this paper is an according vibration attenuation at the engine mounting by actively controlled force actuators. In car industry, sophisticated passive methods are already extensively applied for engine vibration isolation and semi active methods are focus of current development. However, the possible benefits of active systems, like flexibility and high effectiveness, are rarely utilized. One of the main reasons for this is the potentially high power consumption of active systems. Aim of this paper is therefore an estimation of the power demands to be expected and to determine an actuator arrangement which promises minimal energy needs.

For the analysis of power demands, an experimental setup is considered which is introduced in the following section. Furthermore, physical models for the dynamic behavior of the mechanical system and the used actuators are presented. The corresponding mathematical modelling is described in Section 3 as well as a derivation of frequency dependent formulas for the calculation of power demands. The results for the given application are shown and discussed in Section 4, followed by a conclusion in the last section.

2. MECHANICAL SETUP, ACTUATORS AND PHYSICAL MODELING

The mechanical system of interest is the mounting of an automobile engine on the cars chassis. The considered experimental setup is shown in Figure 1. An actuator

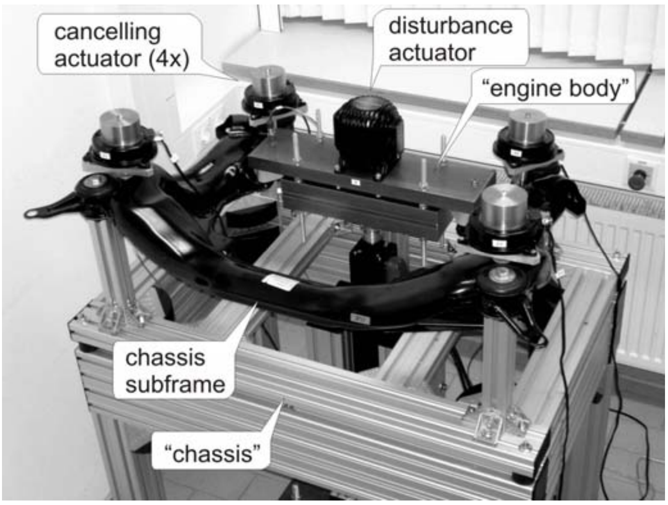

Figure 1 – Experimental setup

attached to a mass representing the engine body is used to excite the system mechanically. The mass is mounted at two points to a so called chassis subframe. The subframe itself is mounted at four points to a base framework which stands for the cars chassis. The chassis subframe is a U-shaped, hollow steel body. It is considered to be rigid for the following estimation of power demands. The engine mass and the chassis subframe as well as the underlying "chassis" are connected by rubber mounts. Their spring and damping characteristics are assumed to be linear for the following analysis. Thus, the physical model shown in Figure 2 a) and b) can be derived for the setup. In the model, the spring and damping properties of the mounts are cumulated to the spring constants c_i and damping constants d_i.

In Figure 2 a) and b), two kinds of actuator principles are presented that are considered for the power analysis: The first one is that of a reaction mass actuator (as installed on the experimental setup depicted in Figure 1) where the force actuator is built in between the mass to be attenuated and an additional mass m_A. In that way, a compensation of applied forces is accomplished. For the second principle, the force actuator is installed directly between two masses of the setup. This achieves a

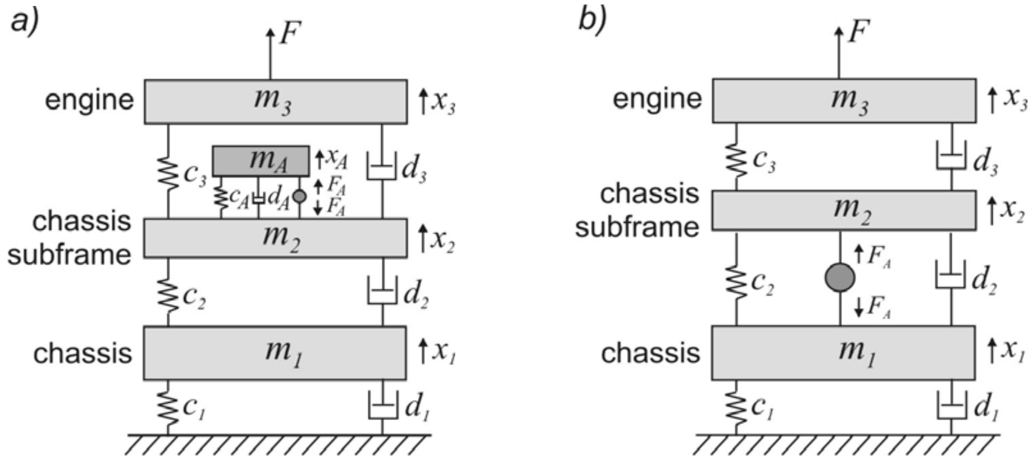

Figure 2 – Physical model of the engine mounting with
a) force compensation, b) displacement compensation

compensation of the displacement of the body. At the experimental setup shown in Figure 1, only the actuator principle for force compensation has already been realized for the possible actuator configurations. A multi-channel feedforward system [3]−[5] is used as control system. However, the displacement compensation will as well be subject to the following theoretical analysis.

The considered force actuators are of voice coil type. They are physically modelled as shown in Figure 3. In the model in Figure 2, the four real actuators are replaced by a single one with four times the original values of mass as well as spring and damping constants. The values of resistance *R* and inductance *L* are a quarter of the original ones. Voltages and other parameters remain unchanged.

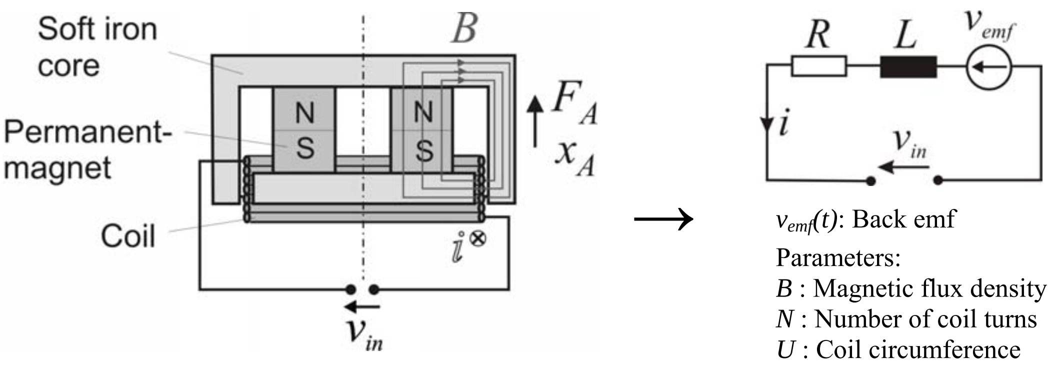

Figure 3 – Physical model of the force actuator

With the two different kinds of actuator principles applied to the basic three-body model in Figure 2, six configurations of actuator placement are possible. Figure 4 illustrates them schematically together with the shortcuts used in the following text. It can be presumed that the configuration *m3A* is disadvantageous regarding energy demands: Since there are no intermediate passive damping elements, the actuators have to compensate for the complete accelerating forces at the engine body.

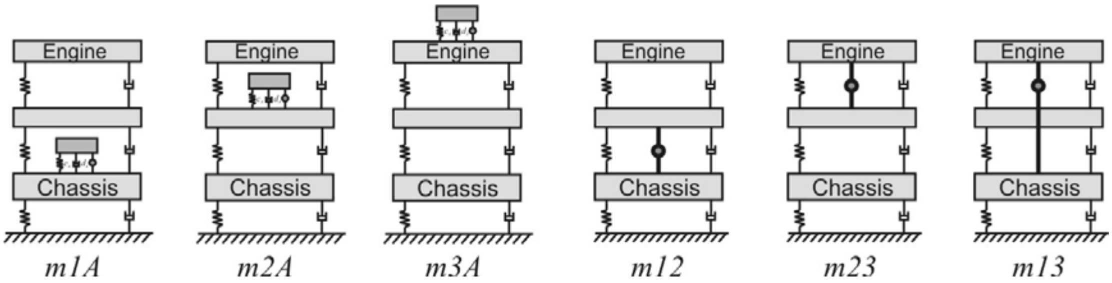

Figure 4 – Possible actuator configurations

Furthermore, the configuration *m13* is not suitable for the given structure geometry. In this arrangement (just as for *m3A* and *m23*) only two force actuators can be mounted. Since the engine is not symmetrically mounted to the chassis subframe, rotatory modes of the subframe are excited which can not be completely compensated for by just two actuators between *m1* and *m3*.

3. MATHEMATICAL MODELLING AND POWER DEMAND

For a thorough analysis of the different actuator arrangements, mathematical models of the corresponding overall setups are necessary. The modelling of the mechanical part can be done by applying Newton's second law. The force actuator model of Figure 3 is connected by the Lorentz force $F_A(t)$ and the back emf $v_{emf}(t)$. Exemplary, the resulting set of equations for the configuration depicted in Figure 2 a) is:

Mechanical:

$$\begin{aligned} m_1\ddot{x}_1(t) &= -c_1x_1(t) - d_1\dot{x}_1(t) + c_2(x_2(t)-x_1(t)) + d_2(\dot{x}_2(t)-\dot{x}_1(t)) \\ m_2\ddot{x}_2(t) &= -c_2(x_2(t)-x_1(t)) - d_2(\dot{x}_2(t)-\dot{x}_1(t)) + c_3(x_3(t)-x_2(t)) \\ &\quad + d_3(\dot{x}_3(t)-\dot{x}_2(t)) + c_A(x_A(t)-x_2(t)) + d_A(\dot{x}_A(t)-\dot{x}_2(t)) - F_A(t) \\ m_3\ddot{x}_3(t) &= -c_3(x_3(t)-x_2(t)) - d_3(\dot{x}_3(t)-\dot{x}_2(t)) + F(t) \end{aligned} \tag{1}$$

Electrical:

$$v_{in}(t) = L\frac{di(t)}{dt} + R\,i(t) + v_{emf}(t) \tag{2}$$

Connecting equations:

$$F_A(t) = BNU\,i(t)\,, \qquad v_{emf}(t) = BNU(\dot{x}_A(t)-\dot{x}_2(t)) \tag{3}$$

For further analysis of the system, the describing equations are transformed into the Laplace domain. Initial values are set to zero. An estimation of power demands is derived by assuming a complete vibration cancellation for the body the actuator is mounted on. In practice a nearly perfect suppression can be achieved by feedforward algorithms. These work highly effective over the complete frequency range of interest [3]−[5]. The assumption is implemented by setting the displacement value of the body to zero in the Laplace domain. Thus, also the order of the overall system is decreased. For a frequency related analysis, transfer functions from the excitation force $F(t)$ to the output variables of interest can be derived. Four transfer functions are needed in particular for the following estimation of power demands:

$$\begin{aligned} &G_{F_A}(s) &&: F(s) \rightarrow \text{actuator force } F_A(s) \\ &G_{\dot{x}_A}(s) &&: F(s) \rightarrow \text{actuator velocity } \dot{x}_A(s) \\ &G_{v_{in}}(s) &&: F(s) \rightarrow \text{actuator input voltage } v_{in}(s) \\ &G_i(s) &&: F(s) \rightarrow \text{current through actuator coil } i(s) \end{aligned} \tag{4}$$

The instantaneous mechanical power consumption is calculated by

$$P_{mech}(t) = F_A(t) \cdot (\dot{x}_A(t) - \dot{x}_2(t)), \quad \dot{x}_2(t) = 0 \tag{5}$$

and the instantaneous electrical power consumption by

$$P_{el}(t) = v_{in}(t) \cdot i(t) \quad . \tag{6}$$

If the excitation force is assumed to be harmonic ($F(t) = |F| \cos(\omega t)$), numerical values of e.g. the electrical power are obtained by inserting the frequency responses given by (4) in (6):

$$P_{el}(t) = \text{Re}\{G_{v_{in}}(j\omega)|F|e^{j\omega t}\} \cdot \text{Re}\{G_i(j\omega)|F|e^{j\omega t}\}) \tag{7}$$

By transforming the received expression

$$\begin{aligned} P_{el}(t) &= |F|^2 \cdot \text{Re}\{|G_{v_{in}}(j\omega)|e^{j\angle G_{v_{in}}(j\omega)}\, e^{j\omega t}\} \cdot \text{Re}\{|G_i(j\omega)|e^{j\angle G_i(j\omega)}\, e^{j\omega t}\} \\ &= |F|^2 \cdot |G_{v_{in}}(j\omega)| \cdot \cos(\omega t + \angle G_{v_{in}}(j\omega)) \cdot |G_i(j\omega)| \cdot \cos(\omega t + \angle G_i(j\omega)) \\ &= \frac{1}{2}|F|^2 \cdot |G_{v_{in}}(j\omega)||G_i(j\omega)| \cdot [\cos(2\omega t + \angle G_{v_{in}}(j\omega) + \angle G_i(j\omega)) \\ &\qquad + \cos(\angle G_{v_{in}}(j\omega) - \angle G_i(j\omega))] \end{aligned} \tag{8}$$

it becomes obvious, that the electrical power is a superposition of a constant value and a harmonic signal with a frequency twice as high as that of the original excitation signal $F(t)$. The mean value of the power consumption can be calculated by

$$\overline{P}_{el} = \frac{1}{T}\int_{t=0}^{T} P_{el}(t)dt$$
$$= \frac{1}{2}\left|F\right|^2 \cdot \left|G_{v_{in}}(j\omega)\right|\left|G_{v_i}(j\omega)\right| \cdot \cos(\angle G_{v_{in}}(j\omega) - \angle G_i(j\omega)) \quad , \qquad (9)$$

where T is the fundamental period of the vibration. This derivation can be performed in the same way for the average mechanical power $\overline{P}_{mech}$. It must be mentioned, that in practical application formula (9) is in general only valid, if the phase difference between input voltage and current is $\angle G_{v_{in}}(j\omega) - \angle G_i(j\omega) = k \cdot 2\pi$, where k is an integer. Otherwise it must be distinguished whether power supplies with or without energy recovery are used. Energy recovery systems supply energy while $P_{el}(t)$ is positive and recover energy when $P_{el}(t)$ is negative. Without energy recovery, no energy is fed back from the system. In that case, the actual power demands are given by the average positive power which is calculated by

$$\overline{P}_{el}^{+} = \frac{1}{T}\int_{t=0}^{T} P_{el}^{+}(t)dt \quad , \qquad \text{where } P_{el}^{+}(t) = \begin{cases} P_{el}(t) & if\ P_{el}(t) > 0 \\ 0 & else \end{cases} \quad . \qquad (10)$$

For a phase difference $\angle G_{v_{in}}(j\omega) - \angle G_i(j\omega)$ significantly different from $k \cdot 2\pi$, $\overline{P}_{el}^{+}$ can be much greater than $\overline{P}_{el}$. Especially for the voice coil actuators used here, the phase difference is mainly given by the phase characteristic of the electrical system described by (2). For an estimation of the shape of the characteristic, the effect of the back emf $v_{emf}(t)$ can be neglected. The cut-off frequency of the remaining first order system is determined by the quotient R/L. In the given case the cut-off frequency equals about 500*Hz*. For frequencies significantly lower than this, the resulting effect on the average power is small. Comparing calculation shows that for the application at hand the caused deviation of $\overline{P}_{el}$ and $\overline{P}_{el}^{+}$ is negligible in the considered frequency band. Hence the use of driver electronics with energy recovery does not lead to a significant improvement regarding power consumption here.

4. RESULTS

Following from the previous section, the average mechanical and electrical power demands can be described by $\overline{P}_{mech} = G_{mech}(j\omega) \cdot \left|F\right|^2$ and $\overline{P}_{el} = G_{el}(j\omega) \cdot \left|F\right|^2$ with

$$G_{mech}(j\omega) = \frac{1}{2} \cdot \left|G_{F_A}(j\omega)\right|\left|G_{\dot{x}_A}(j\omega)\right| \cdot \cos\left(\angle G_{F_A}(j\omega) - \angle G_{\dot{x}_A}(j\omega)\right) \qquad (11)$$

and $$G_{el}(j\omega) = \frac{1}{2} \cdot \left|G_{v_{in}}(j\omega)\right|\left|G_i(j\omega)\right| \cdot \cos\left(\angle G_{v_{in}}(j\omega) - \angle G_i(j\omega)\right) \quad . \qquad (12)$$

In Figure 5 the characteristic $G_{mech}(j\omega)$ is presented for the six different actuator configurations of Figure 4. The characteristic is scaled to $G_{mech}[dB] = \mathbf{10} \cdot \log_{10}(G_{mech})$. The plot of *m13* is visualised for values up to about $50Hz$ only since $G_{mech}(j\omega)$ is negative for higher frequencies. This indicates a gain of mechanical energy which is an interesting result of the theoretical analysis. The voice coil actuators are not able to utilize this effect but other types of force actuators might be.

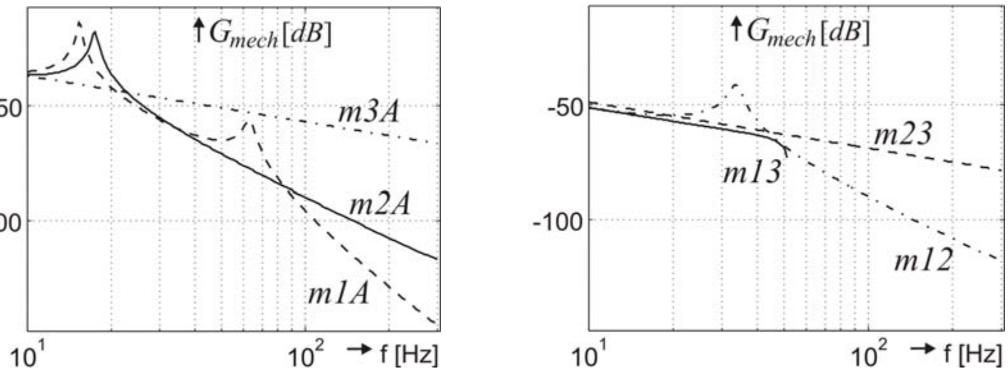

Figure 5 – Transmission of squared force magnitude $|F^2|$ *to average mech. power* $\overline{P}_{mech}$

Figure six shows the characteristics $G_{el}(j\omega)$ of the electrical power consumption. For the application in a real car, the actual amount of power demand is not easy to determine. Beside the depicted characteristics it depends on the excitation force magnitude $|F|$ which is strongly influenced by the considered engine type and its load profile. Nevertheless, for a simplified analysis the integral of $G_{el}(j\omega)$ over the relevant frequency range can be used as a measure for the overall energy demand. In addition to that, the peak value of $G_{el}(j\omega)$ indicates the maximum necessary load limits of the actuators. Taking into account these quality criteria and keeping in mind the logarithmic scaling, Figure 6 shows that the configuration *m2A* is presumably the best solution regarding electrical power demands. Second-best is the arrangement *m1A*.

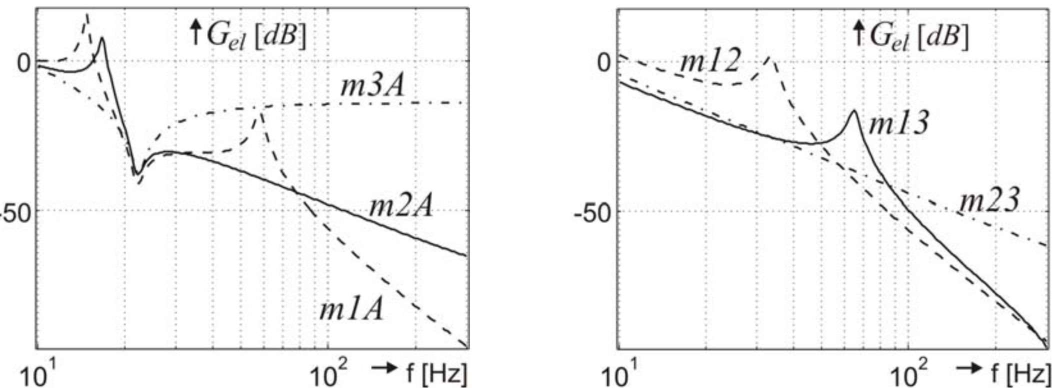

Figure 6 – Transmission of squared force magnitude $|F^2|$ *to average electrical power* $\overline{P}_{el}$

However, at frequencies of around 60*Hz*, $G_{el}(j\omega)$ is much higher for *m1A* than for *m2A*. This is due to the fact that the chassis subframe *m2* is not damped by the active vibration control system and therefore at its resonance frequency causes a high force on the body *m1*.

In Figure 7, the calculated results are compared to measurement data from the experimental setup. Here it can be seen that for *m1A*, besides the mode at about 60*Hz*, another mode of the chassis subframe at about 90*Hz* is excited that is not reproduced by the simple three body model of the engine mounting (Figure 2).

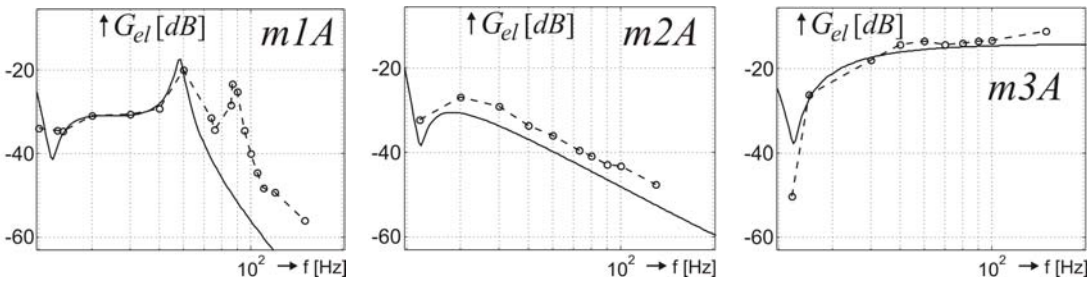

Figure 7 – Comparison of theoretical results and experimental data

5. CONCLUSION

An estimation of the power demands with respect to the possible actuator configurations has been performed for the given automotive application. For the required analysis, an experimental setup has been considered that resembles the real mechanical engine mounting in an automobile. The setup has been modeled together with the installed force actuators. The gained models have been used to derive frequency related characteristics of the mechanical and electrical power demands for force excitation. With these, an optimal actuator arrangement regarding considered criteria has been determined. The obtained results are well matched by measurement data which was gathered by applying a feedforward AVC-system to the experimental setup. However, for one of the configurations, deviations caused by simplified modelling have been detected. Inclusion of system identification methods in the modelling process is a promising approach to eliminate these remaining discrepancies.

REFERENCES

[1] C. Q. Howard, “Active isolation of machinery vibration from flexible structures”, PhD Dissertation, The University of Adelaide, 1999

[2] Y. Yu and N.G. Naganathan, and R.V. Dukkipatit. “Review of automobile vehicle engine mounting systems”, Int. Journal of Vehicle Design, **24**(4), 299 - 319, 2000.

[3] S.M. Kuo, D.R. Morgan, “Active Noise Control Systems”, John Wiley & Sons, New York 1996.

[4] P.A. Nelson and S.J. Elliot, “Active Control of Sound”, Academic Press, London 1992

[5] B. Widrow and S.D. Stearns, “Adaptive Signal Processing”, Prentice Hall, New Jersey 1985.